Science of the Total Environment 947 (2024) 174614

Contents lists available at ScienceDirect

Science of the Total Environment

journal homepage: www.elsevier.com/locate/scitotenv

Effect of boramidic acid modified carbon nanotubes on neurological, morphological and physiological responses of zebrafish (*Danio rerio*) embryos and larvae

Aybek Yiğit [a,*], Mine Köktürk [b], Serkan Yıldırım [c,d], Dilek Nazli [e,f], Metin Kiliçlioğlu [c], Ayse Sahin [f,g], Muhammed Atamanalp [h], Gunes Ozhan [f,g], Nurettin Menges [i,j,**], Gonca Alak [k,***]

[a] Department of Pharmacy Services, Tuzluca Vocational School, Igdir University, TR-76000 Igdir, Türkiye
[b] Department of Organic Agriculture Management, Faculty of Applied Sciences, Igdir University, TR-76000 Igdir, Türkiye
[c] Department of Pathology, Veterinary Faculty, Ataturk University, Erzurum, Türkiye
[d] Department of Pathology, Veterinary Faculty, Kyrgyzstan-Türkiye Manas University, Bishkek, Kyrgyzstan
[e] Izmir International Biomedicine and Genome Institute (IBG-Izmir), Dokuz Eylul University, 35340 Izmir, Türkiye
[f] Izmir Biomedicine and Genome Center (IBG), Dokuz Eylul University Health Campus, Inciralti-Balcova 35340, Izmir, Türkiye
[g] Department of Molecular Biology and Genetics, Izmir Institute of Technology, Urla 35430, Izmir, Türkiye
[h] Department of Aquaculture, Faculty of Fisheries, Ataturk University, Erzurum, Türkiye
[i] Department of Biomedical Engineering, Faculty of Engineering, Necmettin Erbakan University, 42100 Konya, Türkiye
[j] Science Technology Research and Application Center (BITAM), Necmettin Erbakan University, 42100 Konya, Türkiye
[k] Department of Seafood Processing Technology, Faculty of Fisheries, Ataturk University, Erzurum, Türkiye

HIGHLIGHTS

- Carbon nanotubes itself and having etylene diamine moiety increase toxicity and mortality rate on zebrafish
- Carbon nanotubes (CNT and CNT-ED) force larvae for physiological and morphological abnormalities
- Having boramidic acid unit on the carbon nanotube (CNT-ED-BA) decrases the toxicity of CNT and CNT-ED
- Boramidic acid functionality on carbon nanotubes demonstrates encouraging results against in vivo toxicity.
- At higher concentrations, neurophils exhibited less degeneration and necrosis.

GRAPHICAL ABSTRACT

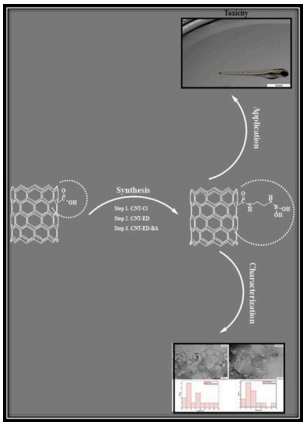

* Correspondence to: A. Yiğit, Department of Pharmacy Services, Tuzluca Vocational School, Igdir University, TR-76000 Igdir, Türkiye.
** Correspondence to: N. Menges, Department of Biomedical Engineering, Faculty of Engineering, Necmettin Erbakan University, 42100 Konya, Türkiye.
*** Correspondence to: G. Alak, Department of Seafood Processing Technology, Faculty of Fisheries, Ataturk University, Erzurum, Türkiye.
E-mail addresses: aybek.yigit@igdir.edu.tr (A. Yiğit), nurettin.menges@erbakan.edu.tr (N. Menges), galak@atauni.edu.tr (G. Alak).

https://doi.org/10.1016/j.scitotenv.2024.174614
Received 3 May 2024; Received in revised form 2 July 2024; Accepted 6 July 2024
Available online 9 July 2024

ARTICLE INFO

Editor: Philiswa Nomngongo

Keywords:
Carbon nanoparticles
Danio rerio
Morphological abnormality
DNA damage
Apoptosis

ABSTRACT

This study aimed to determine the potential toxicological effects of carbon nanotubes (CNTs), their modifications with ethylenediamine (ED) and boric acid (BA) on aquatic organisms. Specifically, the research focused on the morphological, physiological, and histopathological-immuno-histochemical responses in zebrafish (*Danio rerio*) embryos and larvae, via applying different concentrations of CNTs, CNT-ED, and CNT-ED-BA (Control, 5, 10, and 20 mg/L).

The results indicated that 20 mg/L CNT nanoparticles were toxic to zebrafish larvae, with mortality rates increasing with CNT and CNT-ED concentrations, reaching 36.7 % at the highest CNT concentration. The highest dose caused considerable degeneration, necrosis, DNA damage, and apoptosis, as evidenced by histopathological and immunohistochemical tests. In contrast, despite their high concentration, CNT-ED-BA nanoparticles exhibited low toxicity. Behavioral studies revealed that CNT and CNT-ED nanoparticles had a more significant impact on sensory-motor functions compared to CNT-ED-BA nanoparticles. These findings suggest that modifying the nanosurface with boric acid, resulting in boramidic acid, can reduce the toxicity induced by CNT and CNT-ED.

1. Introduction

Hybrid composites made with multiple material components have lately gained major relevance as new-generation materials because of their improved mechanical characteristics (Köktürk et al., 2022; Alak et al., 2023; Ucar et al., 2023; Kokturk et al., 2023). Among these materials, carbon-based nanomaterials (such as carbon black, carbon nanotubes, carbon nanofibers, and graphene) are particularly dominant. Their high porosity and enormous adsorption capacity, resulting from electrostatic interactions with adsorbates, make them highly effective for various important applications, including energy harvesting and storage, sensing, catalysis, transistors, and pollution prevention (Wan et al., 2016).

CNTs, with their one-dimensional tubular shape, are extremely promising within this family because to their quick mass transfer capabilities and enormous specific surface area (Song et al., 2022). Numerous researchers have focused on developing nanotubes catalyzed by transition metals (Fe, Co, Ni), which are excellent catalysts for nanotube synthesis (Niu et al., 2018; Zhang et al., 2022). However, studies on the application of metal-free CNTs are limited, with methods such as chemical vapor deposition (Sawant et al., 2020) and the template method (Wang et al., 2016) being used for synthesis. These methods have disadvantages, such as being time-consuming or requiring additional catalysts. Therefore, investigating more practical methods for synthesizing metal-free doped CNTs is crucial (Liu et al., 2024). Surface modification with natural or synthetic polymers produces more stable hydrophilic nanostructures by increasing the amount of varied functional groups on the surface, which aids in successfully attaching interactomes to the nanostructures.

As the number of products containing nanomaterials increases, so does the potential for organisms in the aquatic biosphere to be exposed to nanoparticles. Aquatic systems can receive nanomaterials from many various sources, such as atmospheric deposition, soil leaching and direct excretions like wastewater discharges. Nanomaterials released into the environment can be transported to aquatic system by effects such as wind and rainwater runoff. The distribution patterns of nanoparticles in the aquatic environment depend on their transport, distribution, transformation and fragmentation after entering the aquatic cascade. Additionally, significant levels of nanomaterials are being intentionally introduced into soil and groundwater through environmental remediation practices (Ateş et al., 2013).

The interaction of CNTs with aquatic environments is a critical topic, yet it remains poorly understood (Audira et al., 2024). Verifying the safety of CNTs in aquatic organisms is essential to address this knowledge gap. The accumulation of these nanomaterials in aquatic environments can pose a threat to aquatic organisms (Ateş et al., 2013). Reactive oxygen species (ROS) generated by nanomaterials can alter the homeostatic redox state of the host. These nanoparticles can enter cells by diffusion or endocytosis, causing mitochondrial dysfunction, protein and nucleic acid damage, inhibited cell proliferation and increased ROS formation, and the increased chemical reactivity of nanomaterials leads to elevated ROS production.

It is well known that an increase in ROS within an organism leads to the accumulation of free radicals. This accumulation is usually toxic due to the oxidation of polyunsaturated fatty acids, proteins, and DNA. ROS can impair cellular defenses, cause DNA chain breaks, and disrupt various biochemical mechanisms (membrane ion transport systems, enzymes, proteins, and lipids). Such damage can result in severe tissue injury due to a disruption in the balance between pro-oxidants and antioxidants (Precourt et al., 2009). Many oxidative DNA damage products have been identified, among which guanine-derived 8-hydroxyguanine (8-OHGua) and 8-hydroxy-2′-deoxynucleoside (8-OHdG) are particularly important for detecting DNA damage. Apoptosis is a normal physiological response to many stimuli, including infections or irreparable DNA damage caused by cytotoxic drugs or radiotherapy. This complex mechanism involves numerous signaling pathways, ultimately activating apoptotic caspases and causing morphological and biochemical cellular changes that initiate apoptosis (Alak et al., 2023).

The behavior of nanoparticles in interaction with surrounding tissues is influenced by their size, shape and surface reactivity. Smaller particles have a larger surface area to volume ratio, resulting in higher chemical reactivity and biological activity. Furthermore, nanomaterials can activate intracellular signaling, inactivate or stimulate enzymes, and trigger the secretion and release of pro-inflammatory cytokines, chemokines and nuclear factors (Altav et al., 2019).

Determining the morphological and physiological effects and biochemical mechanisms in aquatic organisms are important reference processes. Zebrafish (*Danio rerio*) are widely used as model organisms in toxicity tests due to their advantageous characteristics, such as transparent appearance and rapid developmental period during the embryo and larval stages, which allow for the observation of pollutant effects in a short time. Their short life cycles, ease of laboratory maintenance, and ability to produce large numbers of eggs make them increasingly valuable in toxicity tests (Sulukan and Köktürk, 2023).

In recent years, boric acid (BA) and related derivatives, with three hydroxyl groups and modest acidity, have been employed in different composites for reasons such as improving heat resistance, mechanical strength, and gas barrier (Köktürk et al., 2022).

In the present study, CNT-ED-BA was synthesized by chemically modifying CNT-COOH with ED and BA. Behavioral, morphological, and histopathological/immuno-histochemical toxicity assessments were conducted to evaluate the potential use of BA modification in enhancing the electrical conductivity and creating more active sites on the catalyst. Zebrafish embryos and larvae were used as model organisms for these toxicity tests, with implications for clinical diagnostic applications.

2. Materials and methods

2.1. Reagents

Commercially available CNT-COOH (purity >96 %), ethylene diamine (ED, purity 98 %), dimethylformamide (DMF, purity 99 %), tetrahydrofuran (THF, purity 99 %), diethyl ether (purity 99 %), ethyl alcohol (purity 99 %), boric acid (BA, purity 99.5 %), thionyl chloride ($SOCl_2$, purity >99 %) were utilized.

2.2. Synthesis of CNT-ED-BA

Step 1: A 50 mL round-bottom glass flask was filled with 50 mg of multi-walled CNTs (MWCNTs) terminated with carboxylic acid functionality purchased from a commercial source. To this, 10 mL of thionyl chloride ($SOCl_2$) was added and heated for 18 h at 70 °C. After that, 1 mL of anhydrous dimethylformamide (DMF) was added to the mixture, which was stirred for 2 h at room temperature using a magnetic stirrer. Following the stirring procedure, the solid material (CNT-COCl) was filtered (with gooche crucible No. 3) and washed with diethyl ether, THF, and DMF before being dried in an oven at a low temperature.

Step 2: 50 mg of CNT-COCl and 4 mL of ethylene diamine were combined in a 25 mL round-bottom glass flask. The mixture was then heated at 110 °C for 18 h. After heating, the solid material (CNT-ED) was filtered (with gooche crucible No. 3), washed with diethyl ether, THF, DMF, and dried in an oven at low temperature.

Step 3: 50 mg of CNT-ED and 150 mg of boric acid were mixed with 5 mL of anhydrous DMF in a 25 mL round-bottom glass flask. The mixture was then heated for 18 h at 150 °C. The resultant solid material (CNT-ED-BA) was filtered (with gooche crucible No. 3) and washed with DMF, THF, and diethyl ether before drying in an oven at a low temperature (Fig. 1).

2.3. Characterization of CNT-ED-BA

PerkinElmer Spectrum Two FT-IR (Fourier transform infrared) spectrophotometer (PerkinElmer, MA, US) equipped with a potassium bromide (KBr) beam splitter was used to characterize the functional modifications made on the surface of CNTs. To determine the size and crystallographic structure of the modified samples, X-ray diffraction (XRD) analysis was performed using an X-ray diffractometer Panalytical Empyrean (Malvern Panalytical, Malvern, UK). Morphological changes on the surface were imaged using a ZEISS GeminiSEM 500 field emission scanning electron microscope (FESEM; Carl Zeiss AG, Jena, Germany) operating at 10 kV voltage and 1000× magnification. For detailed morphological, structural and dimensional analysis of the particles, the Hitachi HT7800 transmission electron microscope (TEM; Hitachi, Tokyo, Japan) was utilized, operating at 100 kV voltage and providing up to 150.000× magnification.

2.4. Zebrafish maintenance, embryo collection and exposure to nanoparticles

The study was conducted at Izmir Biomedicine and Genome Center, where wild-type (wt) AB zebrafish embryos were utilized. Broodstock zebrafish were maintained according to the standard procedures, with a temperature of 28 °C and a photoperiod of 14 h light to 10 h dark, and fed a diet of flake food and Artemia (Köktürk et al., 2023). For spawning, adults were placed in spawning tanks the day before the experiment with a 1:1 female to male ratio. The next morning, when the lights were turned on, the barrier between the male and female fish was removed. After spawning, embryos were collected and transferred to petri dishes containing E3 medium (0.17 mM KCl, 0.33 mM $MgSO_4$, 5 mM NaCl, and 0.33 mM $CaCl_2$) and maintained at 28 °C (Köktürk et al., 2022). Ethical approval was not required as the study used larvae younger than five days old (Directive 86/609/EEC and EU Directive 2010/63/EU).

To determine the toxicity of the CNT-ED-BA nanoparticles, dose determination was based on toxicity studies of CNT nanoparticles in zebrafish embryos (Aksakal et al., 2019; Falinski et al., 2019). The solutions of CNT, CNT-ED, and CNT-ED-BA nanoparticles were prepared by diluting from a stock solution at 100 mg/L to concentrations of 5, 10, and 20 mg/L. The stock solutions/dilutions were prepared in E3 medium and sonicated using a Minichiller Diagenode sonicator at 50/60 kHz (Huber, Germany) for 10 min to ensure homogeneity. Throughout the experimental period, solutions were sonicated again daily to prevent nanoparticle agglomeration. For each experimental group, 20 zebrafish embryos were used, and the experiment included 3 replicates. Nanoparticle exposure was initiated 4 h post-fertilization (hpf) and continued until 96 hpf in an incubator maintained at 28 °C.

2.5. Acute toxicity assessment: mortality, hatchability, and malformation

To determine the acute toxicity of nanoparticles in embryos and larvae, several parameters were monitored and photographed over specific time intervals. A SZX16 stereomicroscope equipped with an SC50 Olympus camera (Olympus Corporation, Tokyo, Japan) was used for the documentation of these parameters. Mortality rates were assessed at 24, 48, 72 and 96 hpf. The hatching rate was evaluated at 48, 72 and 96 hpf. Morphological changes were observed and documented at 24, 48, 72 and 96 hpf.

2.6. Behavioral assessment: sensory-motor reflexes

Sensory-motor reflexes were analyzed at 96 hpf to examine the effects of nanoparticles on behavior. The head and tail of 5 embryos (n = 3) from each group were touched 10 times at 30 s intervals. The positive immediate swimming behavior and negative immobilization behavior reflexes of the larvae were recorded. A micropipette was used to touch the head and tail of the larvae (Cunha et al., 2018; Rodrigues et al., 2020).

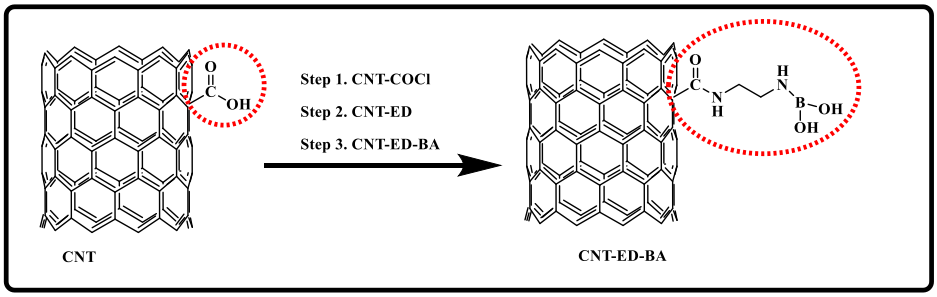

Fig. 1. Schematic representation of the synthesis stages of CNT-ED-BA.

2.7. Histopathological examination

After the exposure to nanoparticles was terminated at 96 hpf, 10 larvae from each treatment group were fixed in 4 % formaldehyde solution for 48 h. Brain tissue samples were then embedded in paraffin blocks following routine tissue processing procedures. Sections of 4 μm thickness were taken from each block, stained with hematoxylin-eosin (HE) and examined under a BX51 microscope (Olympus Corporation, Tokyo, Japan). The sections were evaluated based on histopathological features and categorized as absent (−), mild (+), moderate (+++), and severe (++++).

2.8. Double immunofluorescence examination

For the double immunofluorescent staining, tissue sections mounted on adhesive poly-L-lysine slides were deparaffinized and dehydrated. Endogenous peroxidase was inactivated by incubation in 3 % H_2O_2 for 10 min. Antigen retrieval was performed by boiling the tissues in a 1 % antigen retrieval solution (citrate buffer, pH 6.1, 100×) and allowing them to cool to room temperature. To prevent nonspecific background tissue staining, the sections were incubated with a protein block for 5 min. The primary antibody 8-OHdG (Cat No: sc-66036, 1:100; Santa Cruz Biotechnology, TX, US) was then applied to the tissues and incubated according to the manufacturer's instructions. The sections were then incubated with a goat anti-mouse IgG secondary antibody conjugated with FITC (Cat No: ab6785, 1:1000; Abcam, Cambridge, UK) in the dark for 45 min. The next primary antibody caspase-3 (Cat No: sc-56053, 1:100, Santa Cruz Biotechnology, TX, US) was applied and incubated as per the instructions. Afterwards, the sections were incubated with a goat anti-rabbit IgG H&L secondary antibody conjugated with Texas Red® (Cat No: ab6719, 1:1000; Abcam, Cambridge, UK) in the dark for 45 min. Finally, sections were counterstained with DAPI (Cat no: D1306, 1:200; Thermo Fisher Scientific, MA, US) in the dark for 5 min, and covered with coverslips. The stained sections were examined under a ZEISS Axio Observer fluorescence microscope (Carl Zeiss AG, Jena, Germany). Measurements were taken using the ZEISS Zen Imaging Software, and scores were determined according to the wavelength of the positive incident radiation.

2.9. Statistical analysis

The morphological and behavioral data were statistically evaluated using GraphPad Prism 8 (GraphPad Software, MA, US). All results were presented as mean ± standard deviation (SD), with differences considered statistically significant at ****$p < 0.0001$, ***$p < 0.001$, **$p < 0.01$, and *$p < 0.05$. Differences in mortality, morphological abnormality rates and sensory-motor reflexes were assessed using one-way ANOVA followed by multiple comparison tests (Tukey test for mortality and morphological abnormality rates, and Dunnett's test for sensory-motor reflexes). Hatching rate data were assessed using a two-way ANOVA approach followed by the Dunnett's test.

Graph Pad Prism 8.0.2 was used for statistical analysis in histopathological examinations, with $p < 0.05$ considered significant. Comparisons between groups were performed using the Duncan test. The nonparametric Kruskal-Wallis test was used to determine group interactions, and the Mann-Whitney *U* test was used to determine differences between groups.

To determine the intensity of positive staining in the images obtained from immunofluorescence staining, 5 random areas were selected from each image and evaluated using the ZEISS Zen Imaging Software. Data were statistically described as mean ± SD for the percentage area. One-way ANOVA followed by the Tukey test was performed to compare positive immuno-reactive cells and immuno-positive stained areas with healthy controls. A p value < 0.05 was considered significant.

3. Results

3.1. Characterization of CNT-ED-BA nanoparticles using FT-IR, XRD, FE-SEM, and TEM

Fourier transform infrared (FT-IR) spectra of CNT-ED revealed characteristic vibrational bands between 2500 and 3000 cm^{-1}, indicative of amine groups (—NH_2). A strong vibrational band between 1500 and 2000 cm^{-1} was identified, corresponding to the carbonyl group of the amide functional group (—C═O). In addition, vibration between 500 and 1500 cm^{-1} was attributed to C—N functionality. On the other hand, in the FT-IR spectrum of CNT-ED-BA, the amine groups (—NH) were identified by a vibrational band between 3000 and 3500 cm^{-1}. The carbonyl group associated with the amide functional group (—C═O) was observed in the vibrational band between 1500 and 2000 cm^{-1}. This band was paired with a strong vibrational band for B—O found between 1000 and 1500 cm^{-1} (Liu and Ye, 2009; Ferreira et al., 2015; Maleki et al., 2017; Rahimi et al., 2019; Irani et al., 2017; Amudi et al., 2023) (Fig. 2).

The modification of the MWCNT surface with amine group was analyzed using X-ray diffraction (XRD). The XRD results showed that the characteristic lattice plane structure of the CNTs was indicated by strong diffraction peaks at $2\theta = 23°$ and $2\theta = 26°$. The modification with ED did not significantly alter the crystal shape and cylindrical wall structure, suggesting that the overall structure of MWCNTs remained intact post-modification (Zhang et al., 2005; Shen et al., 2007; Irani et al., 2017; Zohdi et al., 2019). Following the amine modification, further surface modification with BA was performed. XRD analysis of this BA-modified surface revealed additional diffraction peaks at $2\theta = 30°$ and $2\theta = 32°$, while the strong diffraction peak at $2\theta = 24°$ continued to correspond to the lattice structure of the CNTs. The introduction of boron to the surface was also responsible for the lower intensity diffraction points observed (Han et al., 1999; Sankaran and Viswanathan, 2007; Handuja et al., 2009; Yigit et al., 2021; Amudi et al., 2023) (Fig. 3).

The results from FE-SEM images revealed that amine group modification did not significantly alter the tubular morphology of CNTs (Irani et al., 2017; Khalili et al., 2013; Lee et al., 2015; Rahimi et al., 2019; Yigit et al., 2021). In contrast, CNTs modified with BA exhibited an irregular stacked form (Gajhede et al., 1986; Sankaran and Viswanathan, 2007; Yigit et al., 2021; Amudi et al., 2023). The FE-SEM-EDAX (energy-dispersive X-ray analysis) indicates the percentage

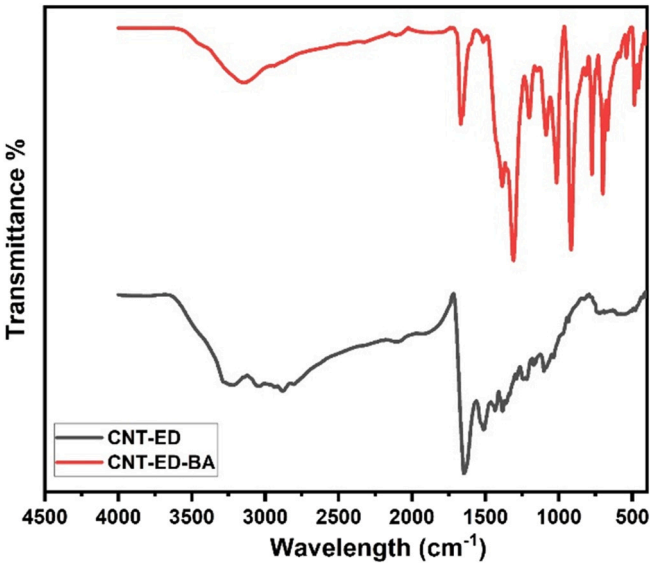

Fig. 2. FT-IR spectra of multi-walled carbon nanotubes (MWCNTs) modified by amine (CNT-ED) and boric acid (CNT-ED-BA).

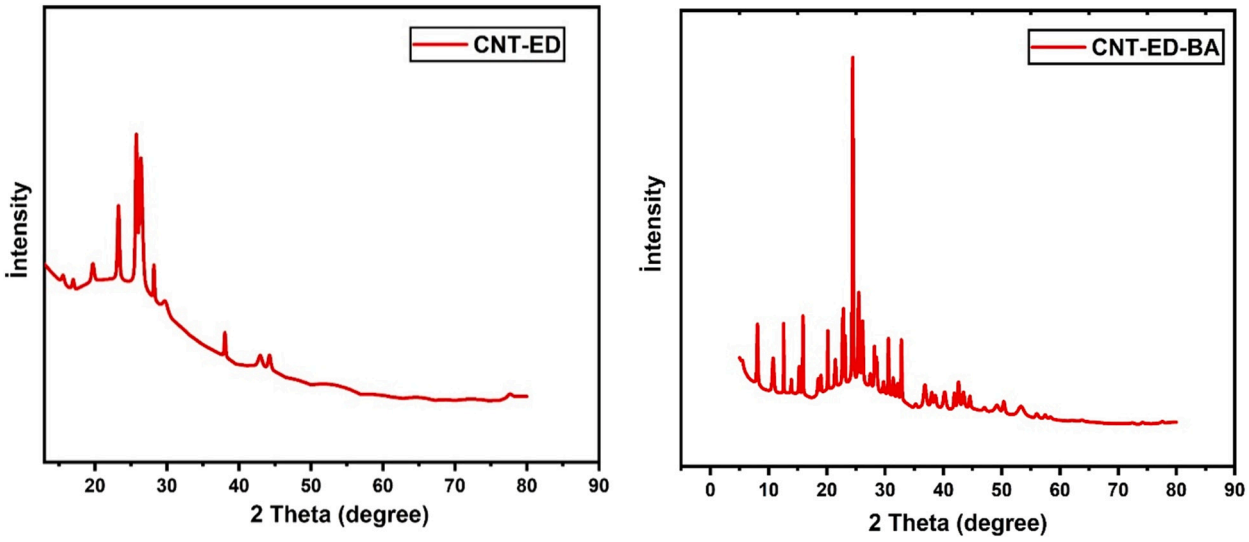

Fig. 3. XRD patterns of the surfaces of multi-walled carbon nanotubes (MWCNT) modified with amine groups (CNT-ED) and boric acid (CNT-ED-BA).

distribution of the structure's constituents. For CNT-ED, the elemental composition was 57.69 % carbon (C), 29.35 % nitrogen (N), and 11.03 % oxygen (O). For CNT-ED-BA, the composition shifted to 25.12 % C, 13.33 % N, and 61.15 % O. Spectral analysis confirms the presence of boron; however, its quantity is challenging to determine due to its atomic number being close to that of C (Cui et al., 2015; Maleki et al., 2017; Junaid et al., 2020; Amudi et al., 2023) (Fig. 4).

TEM imaging of the CNTs modified with ED showed the formation of a thin coating surrounding the tube, without any visible distortion to the tube's morphological structure. The mean particle size for CNT-ED, as measured using image software, was 8.10193 ± 4.29226 nm (Min-Max, 2.703-16.792). In the case of BA modification following the amine group, the tubular structure remained unchanged, though a white lump formed around the tube. The average particle size for this modification (CNT-ED-BA) was 6.40333 ± 3.05629 nm (Min-Max, 2.564–14.704). The pipe diameter appeared slightly reduced with the BA modification performed after the amine group (Redlich et al., 1996; Yang et al., 2009; Silva et al., 2012; Huang et al., 2013; Sharma et al., 2019; Köktürk et al.,

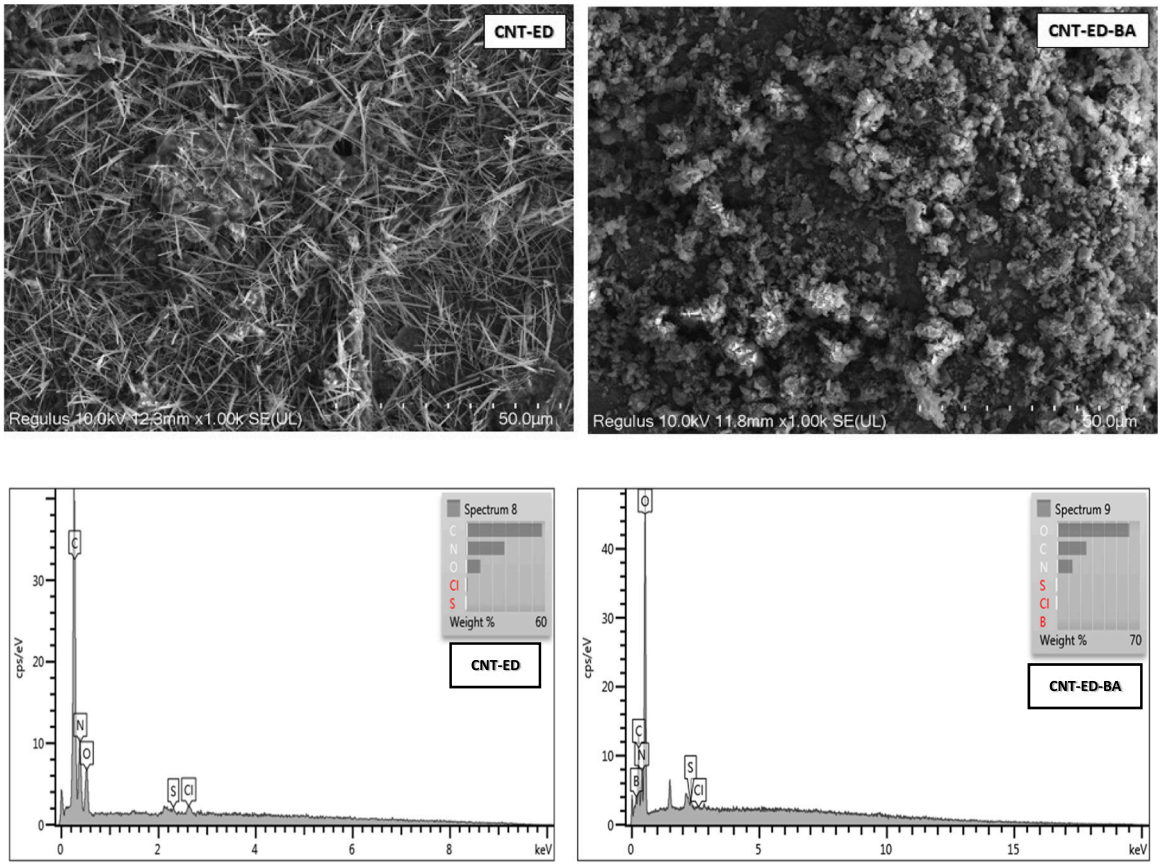

Fig. 4. FE-SEM and FESEM-EDAX images of surface of carbon nanotubes modified by amine (CNT-ED) and boric acid (CNT-ED-BA).

2022; Amudi et al., 2023) (Fig. 5).

3.2. Analysis of mortality, hatching rate and morphological abnormalities in zebrafish larvae exposed to CNTs

To determine the biological toxicity of CNTs in vivo, a series of experiments were conducted in zebrafish. Various concentrations (5, 10, and 20 mg/L) of CNT, CNT-ED, and CNT-ED-BA nanotubes were applied to zebrafish embryos, yielding notable outcomes (Fig. 6). An incremental increase in mortality rates was observed with increasing concentrations of CNT and CNT-ED at 96 hpf (Fig. 6). Notably, increasing concentrations of CNT-ED-BA did not significantly affect mortality rates compared to CNT and CNT-ED.

Larvae normally hatch from the chorion at around 48 hpf, and there was no significant difference in this parameter between the 5 mg/L CNT, and 5 and 10 mg/L CNT-ED-BA groups compared to the control group (Fig. 7). At 72 and 96 hpf, all concentrations in the CNT-ED-BA group produced results equivalent to the control (Fig. 7).

In embryos and larvae, exposure to CNTs (CNT, CNT-ED, CNT-ED-BA) induced morphological deformities, including pericardial edema, spinal curvature, microphthalmia and caudal abnormalities (Fig. 8A). Comparative analysis of morphological abnormality rates with the control group (3.4 %) revealed a significant increase in all treatment groups except for the 5 mg/L (3.7 %) and 10 mg/L (9.4 %) CNT-ED-BA groups (Fig. 8B). The highest incidence of morphological abnormalities was observed in the CNT group at 20 mg/L (29.1 %).

3.3. Exposure to CNTs influence the sensory-motor behavior of zebrafish larvae

To assess the impact of CNT, CNT-ED, and CNT-ED-BA nanoparticles on behavior, a sensory-motor reflex assay was conducted in zebrafish larvae. Upon touching larva's head, there was a noticeable trend towards decreased positive reflexes and increased negative reflexes in all treatment groups except for CNT-ED-BA 5, compared to the control, with statistical significance (Fig. 9). Evaluation of the tactile effect on the tail revealed a statistically significant decrease in positive reflexes and an increase in negative reflexes across all treatment groups except for CNT-ED 5, CNT-ED-BA 5, 10 groups compared to the control (Fig. 9).

3.4. Nanoparticle histopathology and immunohistochemistry findings

Next, to examine the histopathological and immuno-histochemical effects of CNT, CNT-ED and CNT-ED-BA nanoparticles, DNA damage and apoptotic cell death were analyzed on zebrafish larval brain tissues using 8-OHdG and caspase-3, respectively. Immuno-histochemical staining results are provided in Fig. 10, with their quantification shown in Fig. 11. Upon exposure to different concentrations of CNT, CNT-ED, and CNT-ED-BA, varying degrees of degeneration and necrosis in neurophils were observed, as summarized in Table 1.

4. Discussion

Here, we investigate the toxicity of commercially available CNT-COOH and its chemically modified derivatives, CNT-ED and CNT-ED-BA, during the early stages of zebrafish development. To the best of our knowledge, this is the first study to evaluate the behavioral, physiological, histopathological and immuno-histochemical effects of these nanoparticles at different concentrations. After acute treatment, zebrafish larvae emerged from the chorion at 48 hpf. While morphological deformities such as pericardial edema, spinal curvature, microphthalmia, and tail abnormalities were observed in groups treated with CNT and CNT-ED derivatives, CNT-ED-BA appeared to provide protective effects against CNT toxicity. Notably, the observed abnormalities between CNT and CNT-ED varied, with CNT-ED showing more severe effects on zebrafish anatomy. This increased severity could be due to the

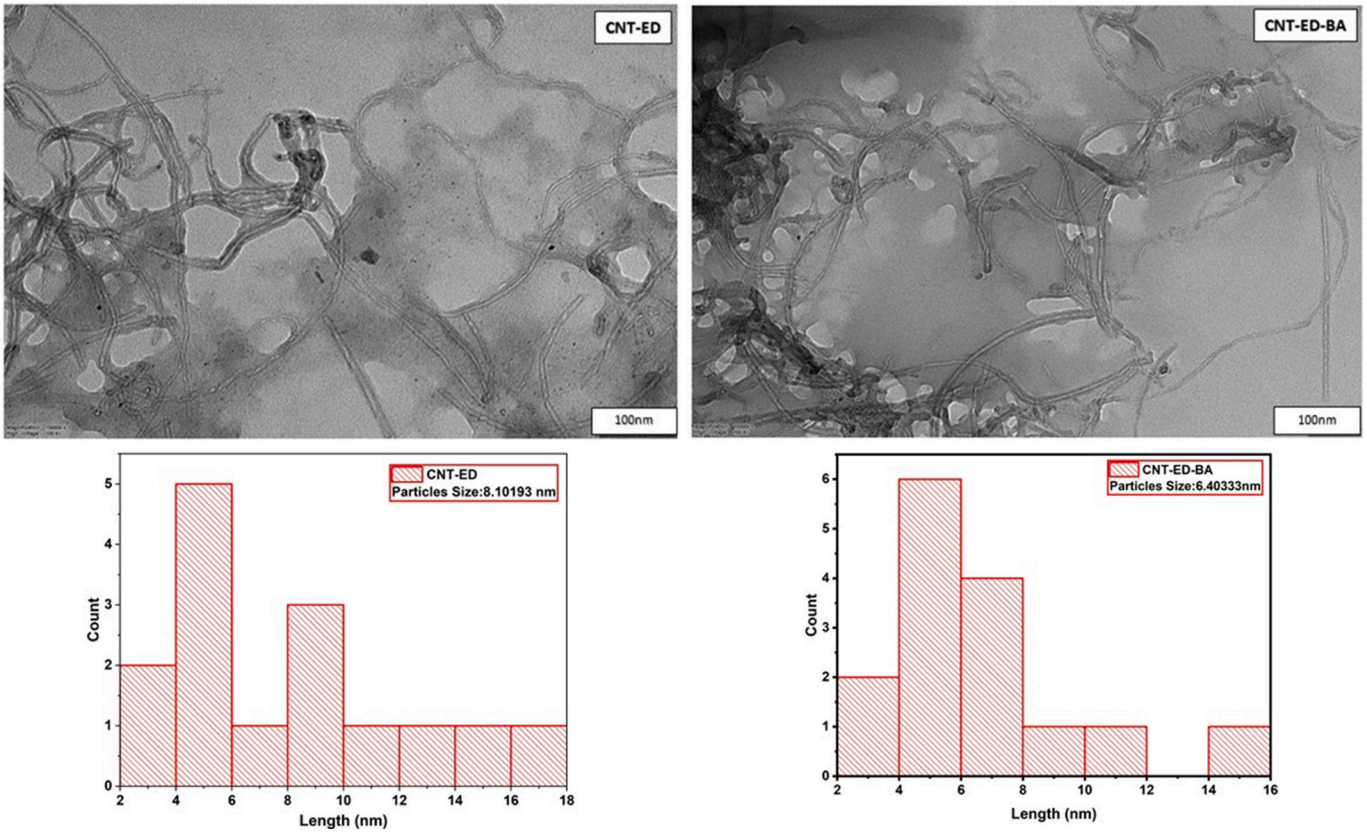

Fig. 5. TEM images and particle size histograms of carbon nanotubes modified by amine (CNT-ED) and boric acid (CNT-ED-BA).

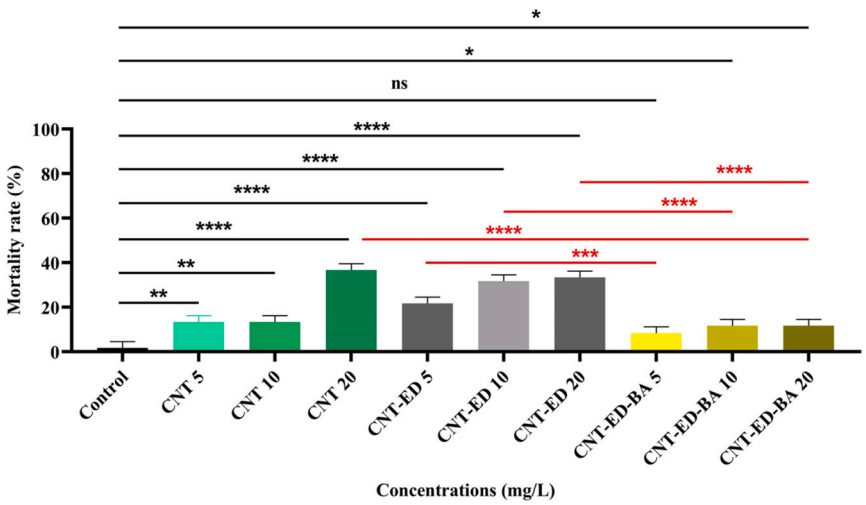

Fig. 6. Mortality rates in zebrafish larvae at 96 hpf following exposure to CNT, CNT-ED and CNT-ED-BA nanoparticles. Statistical significance is indicated as follows: ****p < 0.0001, ***p < 0.001, **p < 0.01, *p < 0.05, and ns: non-significant.

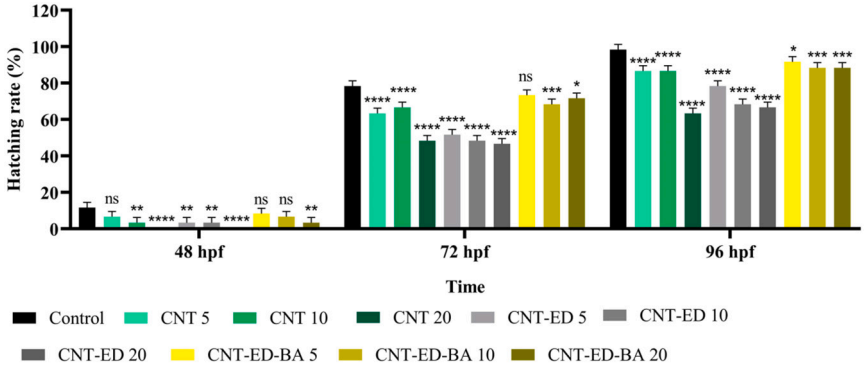

Fig. 7. Chorionic exit rates of zebrafish larvae at 48 hpf, 72 hpf and 96 hpf following exposure to CNT, CNT-ED and CNT-ED-BA nanoparticles. Statistical significance is indicated as follows: ****p < 0.0001, ***p < 0.001, **p < 0.01, *p < 0.05, and ns: non-significant.

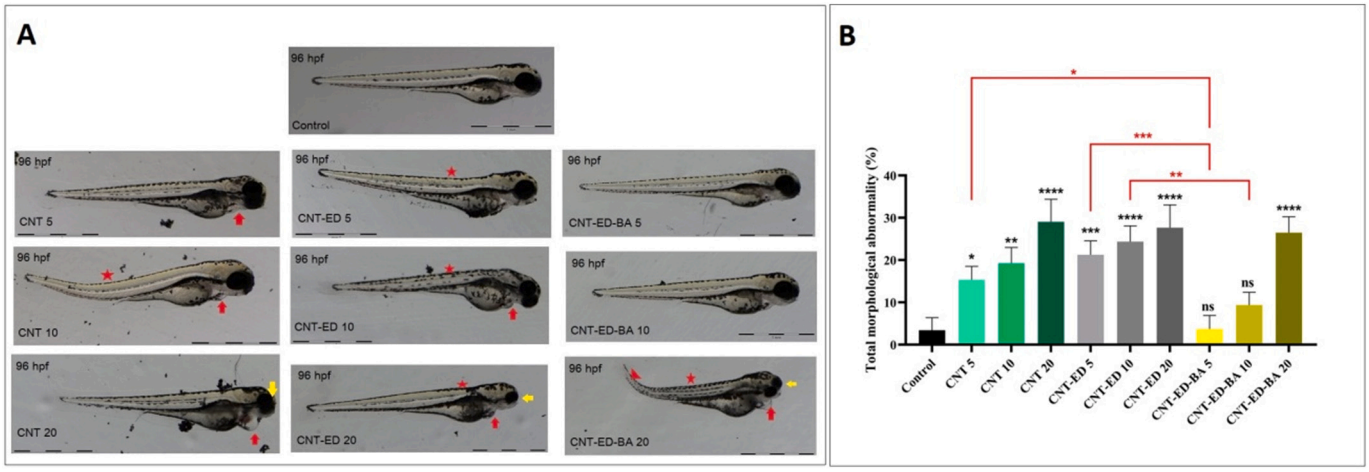

Fig. 8. Morphological abnormalities in the zebrafish larvae following exposure to CNT, CNT-ED and CNT-ED-BA nanoparticles. (A) Bright-field images of larvae at 96 hpf. (B) Total morphological abnormality rates of the larvae. Scale bar: 1 cm. Statistical significance is indicated as follows: ****p < 0.0001, ***p < 0.001, **p < 0.01, *p < 0.05, and ns: non-significant.

free-nucleophilic character of the amine functionality on CNT-ED targeting different endogenous pathways. The highest total morphological abnormalities were seen in CNT-ED 20 and CNT 20, while CNT 10 caused less anatomical damage than CNT-ED10. CNT-ED-BA 5 and CNT-ED-BA 10 had minimal negative impacts on zebrafish anatomy. Behavioral changes in larvae were detected with a sensory-motor reflex. Increased negative reflexes were noted with increasing nanoparticle concentration. CNT-ED 5 or CNT-ED-BA 5 had a beneficial impact on

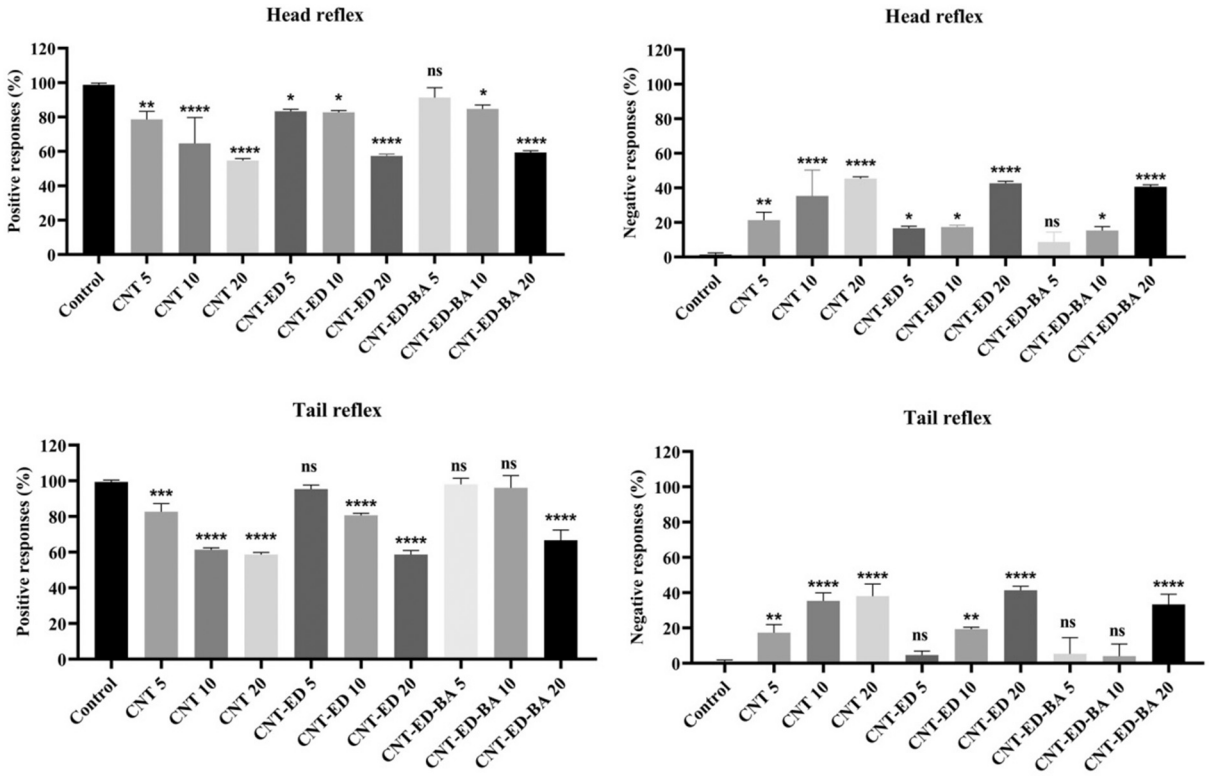

Fig. 9. Head reflex and tail reflex behaviors of 96 hpf zebrafish larvae after exposure to CNT, CNT-ED and CNT-ED-BA. Statistical significance is indicated as follows: ****$p < 0.0001$, ***$p < 0.001$, **$p < 0.01$, ns: non-significant.

head reflexes by up to 80 %. However, CNT 20 and CNT-ED 20 reduced the favorable impact to 54.7 % and 57.3 %, respectively. Similarly, the negative effect of the head reflexes was most pronounced with CNT 20, CNT-ED 20, and CNT-ED-BA 20. At lower concentrations, CNT-ED and CNT-ED-BA produced comparable results. In normally developing larvae not exposed to any chemicals, all larvae moved rapidly away from the stimulus center when the head or tail was touched, indicating active anterior and posterior lateral line systems consisting of neuromasts (Şişman and Geyikoğlu, 2010). However, the most severe negative response, paralysis, was observed in all treatment groups exposed to high doses, potentially due to damage to lateral line systems.

This study applies holistic modeling to determine CNT nanotoxicity or safe doses for aquatic organisms. Toxicological reference indicators such as mortality and hatching rate, malformation, and behavioral changes were evaluated, creating a comprehensive data pool on nanotube-induced developmental toxicities. Dose-dependent increases in mortality and malformations, decreased hatching rates, and altered behaviors indicated that CNT and especially CNT-ED have significant developmental toxicities on zebrafish embryos and larvae. Our findings align with results from other nanoparticle toxicity studies (Aksakal et al., 2019; Köktürk et al., 2022; Kokturk et al., 2023).

Regarding mortality in zebrafish embryos and larvae, CNT-ED-BA was found to be the least toxic modification. Mortality rates for CNT-ED-BA 5, 10, and 20 were 8.3 %, 11.7 %, and 11.7 %, respectively. In contrast, CNT 20 had the highest fatality rate at 36.7 %, with CNT-ED 20 having a comparable rate at 32.8 %. These findings suggest that both CNT and CNT-ED have similar adverse effects causing mortality, likely due to their stringent functionalities targeting endogenous pathways. These results are consistent with literature showing that the functionalization of MWCNTs with various groups (carbonyl, carboxyl, hydroxyl, amino, etc.) significantly impacts their toxicity profile, highlighting the complex role of these modifications in determining toxicity (Chowdhry et al., 2019).

In zebrafish embryos, the chorion serves as the primary defense against the entry of intact nanoparticles. In this study, embryo development in zebrafish remained resistant to increasing concentrations of both intact and functionalized CNT-ED-BA. Such observations align with previous studies showing that some intact and functionalized nanoparticles do not cause significant mortality or malformations in zebrafish embryos (Kokturk et al., 2023). Our previous research demonstrated that graphene oxide-boramidic acid (GO-ED-BA) synthesized with BA similar to CNT-ED-BA, did not adversely affect survival and chorionic outflow success at low doses (Köktürk et al., 2022). In this study, the exit time of zebrafish larvae from the chorion was determined to be 48 h. After 72 and 96 h, all CNT derivatives showed a positive influence on hatchability rates, similar to the control group, with CNT-ED-BA being the most effective derivative at all concentrations. When comparing CNT and CNT-ED for chorionic exit rates, CNT 5 and CNT 10 had a greater influence than CNT-ED 5 and CNT-ED 10. This study suggests that the primer amine units on nanomaterials may not have a favorable effect on exit from the chorion. In contrast to our findings, another study indicated that the deposition of nanoparticles may prevent interactions with zebrafish embryos (Chowdhry et al., 2019). After 72 h of exposure, zebrafish embryos exit the chorion and begin to swim, thus limiting the effective exposure concentration. However, the in vivo role of immune defenses derived from zebrafish embryos cannot be underestimated compared to the in vitro system.

Histopathological research demonstrated that CNT derivatives induced the expression of 8-OHdG and caspase 3 in neuropils. CNT 20, followed by CNT-ED 20, resulted in the highest expression levels of these markers. CNT 5 and 10 as well as CNT-ED 5 and 10 exhibited similar expression rates for these markers. CNT 20 has the most significant effect on both markers compared to other derivatives, which might be due to an unidentified interaction between COOH groups on the nano surface and enzymes residues at different pathways. CNT-COOH has been shown to induce caspase expression (Lotfipanah et al., 2019). Conversely, all CNT-ED-BA concentrations had only a slight effect on marker expression.

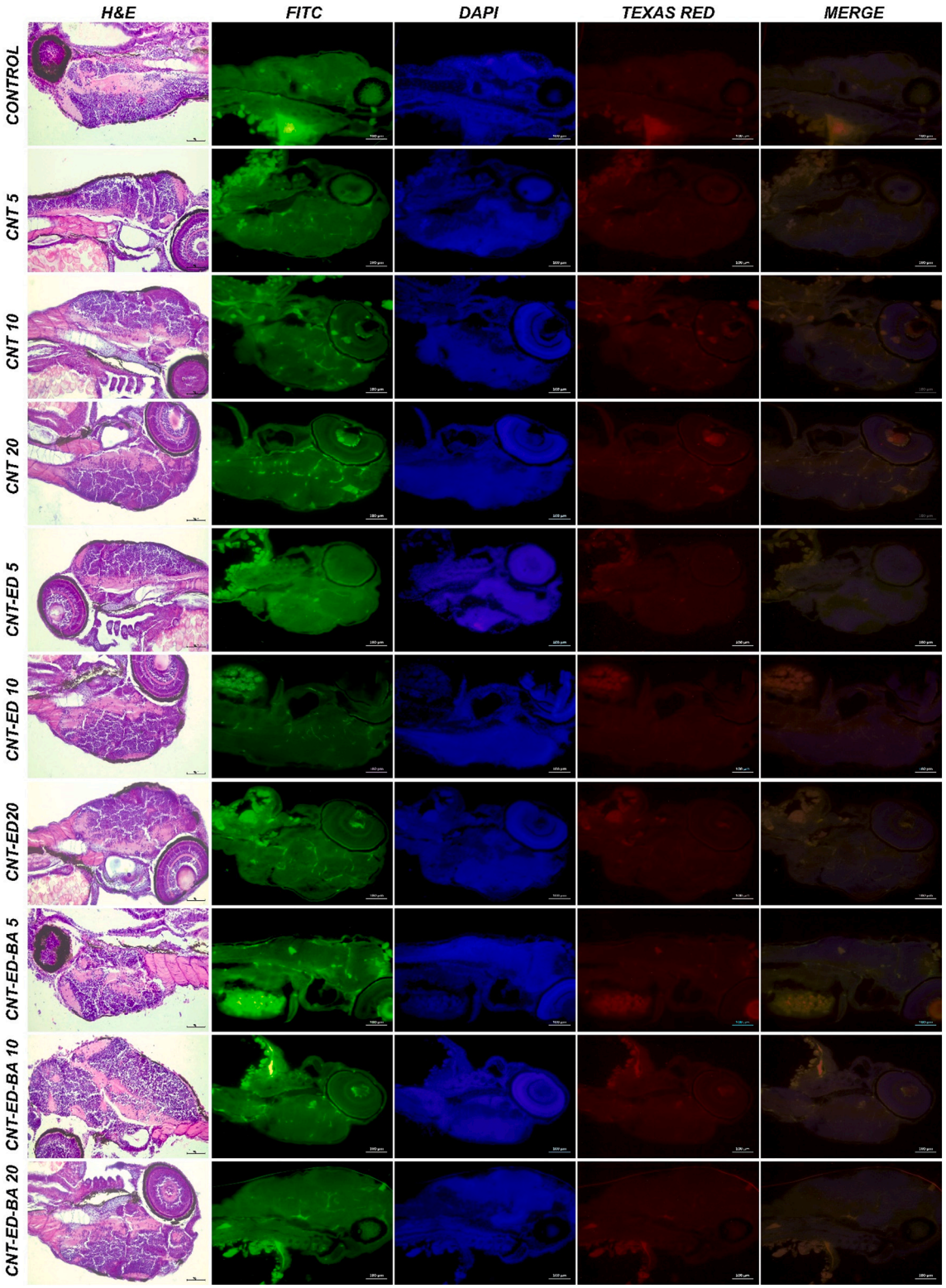

Fig. 10. Microscopic images of hematoxylin and eosin (H&E) and immunofluorescence staining for 8-OHdG (FITC), DAPI, and caspase-3 (TEXAS RED) in brain tissues of zebrafish larvae to exposure to CNT, CNT-ED, and CNT-ED-BA. Scale bars in H&E: 70 μm and in IF: 100 μm.

CNTs can easily pass through cell membranes due to their small size and accumulate in different tissues, causing more toxicity in organisms that remain vulnerable because they are not detected by the immune system (Baughman et al., 2002; Ménard-Moyon et al., 2010). In our study, we found that the multi-walled CNT-ED and CNT-ED-BA nanoparticles, synthesized by modifying CNTs, are smaller than 9 nm in size. These nanoparticles can easily penetrate the tissues, causing varying effects. Previous research has shown that the size of CNTs can decrease when aged by soaking in water, which suggests that CNT-ED and CNT-ED-BA nanoparticles in our study can easily diffuse in the water where they are applied to embryos (Jung et al., 2024). In another study, an interesting aerogel was synthesized from carbon nanotube-enriched

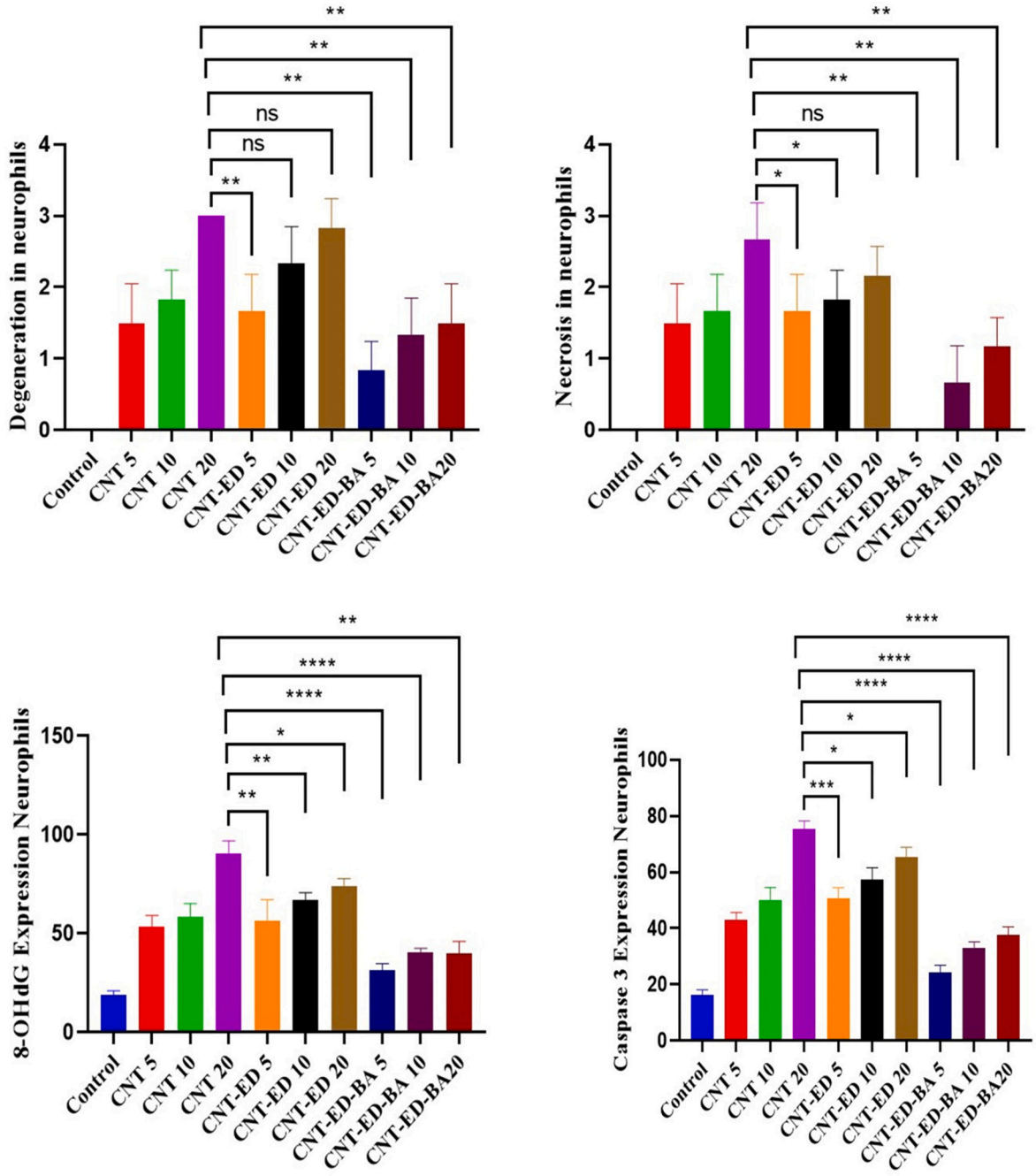

Fig. 11. Analysis of histopathological lesions (degeneration and necrosis of neurophils) and immuno-fluorescent staining (expression levels of 8-OHdG and caspase 3) results in zebrafish larvae brain tissue samples. Neurophil degeneration (**p = 0.0022; ns: non-significant p > 0.005); neurophils necrosis (*p = 0.0325 CNT 20 vs CNT-ED 5; *p = 0.0455 CNT 20 and CNT-ED 10; **p = 0.0022; ns: non-significant p > 0.005); expression levels of 8-OHdG (**p = 0.0031 CNT 20 vs CNT-ED 5; **p = 0.0024 CNT 20 and CNT-ED 10; **p = 0.0011 CNT 20 ve CNT-ED-BA 20; ****p < 0.0001); expression levels of caspase 3 (***p = 0.0002; *p = 0.0102 CNT 20 vs CNT-ED 10; *p = 0.0410 CNT 20 and CNT-ED 20; **p = 0.0011 CNT 20 and CNT-ED-BA 20; ****p < 0.0001).

amino-functional graphene by adding CNTs to graphene oxide solution (John et al., 2021). This aerogel demonstrated an improved microstructure and enhanced chemical and physical adsorption due to the -NH_2 groups in the graphene layer, indicating its potential in various sectors.

CNTs, which have a wide range of uses, can accumulate in the environment and, consequently, in living organisms. In aquatic environments, they can be adsorbed by vertebrate and invertebrate organisms through suspended particles and trophic transitions (Aksakal et al., 2019). Therefore, it is crucial to determine the eco-toxicity of the synthesized substances for acute and chronic processes to ensure their safe use. Zebrafish is often preferred in such studies as a widely used model organism that provides successful results in evaluating the toxicity pathways and mechanisms of nanotubes in terms of physiology and metabolism (Köktürk et al., 2022; Alak et al., 2023; Ucar et al., 2023; Kokturk et al., 2023). A study investigating the effect of surface functionalization with ED on the cytotoxicity profile of CNTs used dual covalent modification of CNTs with carboxy and amino groups (Chowdhry et al., 2019). This modification positively impacted the viability of human embryonic kidney cells (HEK 293) and showed promising results in terms of ROS production profiles.

The safety of CNTs for organisms is controversial, and extensive

Table 1
Histopathological and immuno-histochemical interpretations of synthesized nanoparticles.

Group	Histopathologic findings (Fig. 10)	Immunofluorescence findings (Fig. 10)
Control	Normal histological structure.	No expression of 8-OHdG and Caspase 3 in neurophils.
CNT 5	Moderate degeneration and mild necrosis of neurophils.	Moderate expression of 8-OHdG and Caspase 3 in neurophils.
CNT 10	Moderate degeneration and necrosis of neurophils.	High expression of intracytoplasmic 8-OHdG and Caspase 3 in neurophils.
CNT 20	Severe degeneration and necrosis of neurophils.	Very high expression of cytoplasmic 8-OHdG and Caspase 3 in neurophils.
CNT-ED 5	Moderate degeneration and necrosis of neurophils.	Moderate expression of 8-OHdG and Caspase 3 in neurophils.
CNT-ED 10	Severe degeneration and moderate necrosis of neurophils.	High expression of cytoplasmic 8-OHdG and Caspase 3 in neurophils.
CNT-ED 20	Severe degeneration and moderate necrosis of neurophils.	High expression of intracytoplasmic 8-OHdG and Caspase 3 in neurophils.
CNT-ED-BA 5	Mild degeneration of neurophils.	Very mild expression of 8-OHdG and Caspase 3 in neurophils.
CNT-ED-BA 10	Mild degeneration and necrosis of neurophils.	Mild expression of 8-OHdG and Caspase 3 in neurophils.
CNT-ED-BA 20	Mild degeneration and necrosis of neurophils.	Mild expression of 8-OHdG and Caspase 3 in neurophils.

research has been conducted in recent years. It has been reported that the biocompatibility of CNTs can be enhanced and tissue damage reduced through functionalization and protein binding (Zhao et al., 2024). Our findings indicate that the CNT-ED-BA derivative reduced apoptosis in brain tissue compared to CNT and CNT-ED derivatives. This suggests that BA has ROS scavenging roles and provides tissue protection against apoptosis (Yigit et al., 2021). In this study, the caspase-3 level in CNT-ED-BA was found to be lower than in the other derivatives. This may be due to the suppression of p53-dependent apoptosis, which plays a crucial role in the apoptosis mechanism (Cao et al., 2019; Mehrbeheshti et al., 2022).

When analyzing all the CNT derivatives in this study, we can conclude that the lower toxicity of CNT-ED-BA is likely due to presence of BA. BA has a soft acidic character and its interactions with protein residues are minimal, which might explain its lower toxicity. Additionally, BA is a prominent functionality for substitutions and new chemical modifications. Some studies with zebrafish have shown that BA and its derivatives have protective features (Alak et al., 2020, 2021; Köktürk et al., 2022). Boron and its derivatives are effective in the activity of many enzymes, hormone and lipid metabolism, and can be used safely in aquatic environments (Türkez et al., 2013; Turkez et al., 2021; Alak et al., 2021). Our findings indicate that CNT and CNT-ED induced greater oxidative and genotoxic stress in cells compared to the BA-modified derivative. Consistent with these observations, CNT-induced stress increases DNA damage and apoptosis levels (Köktürk et al., 2022).

5. Conclusion

In this study, we have shown that CNT-ED-BA nanostructures formed after functionalization of the nanosurface first with ED and then with BA are water soluble and biocompatible. Our findings showed that the BA derivatization of nanotube surface had a mitigating effect in reducing CNT-induced toxicity in zebrafish. Moreover, 5 mg/L of CNT-ED-BA was determined to yield better results and could be used safely and effectively. However, the morphological and physiological changes caused by CNT in aquatic organisms, especially in fish, and their role in DNA damage and apoptosis need further investigation. Additional metabolic and nutrigenomic studies are also needed to elucidate the exact mechanisms behind the protective effect of CNT-ED-BA nanoparticles on fish.

CRediT authorship contribution statement

Aybek Yiğit: Writing – original draft, Methodology, Investigation, Formal analysis, Conceptualization. **Mine Köktürk:** Investigation, Formal analysis. **Serkan Yıldırım:** Investigation, Formal analysis. **Dilek Nazli:** Investigation, Formal analysis. **Metin Kiliçlioğlu:** Investigation, Formal analysis. **Ayse Sahin:** Investigation, Formal analysis. **Muhammed Atamanalp:** Writing – review & editing. **Gunes Ozhan:** Investigation, Formal analysis. **Nurettin Menges:** Writing – review & editing, Investigation. **Gonca Alak:** Writing – review & editing, Writing – original draft, Methodology, Investigation, Formal analysis.

Declaration of competing interest

The authors declare that they have no known competing financial interests or personal relationships that could have appeared to influence the work reported in this paper.

Data availability

Data will be made available on request.

References

Aksakal, F.I., Ciltas, A., Ozek, N.S., 2019. A holistic study on potential toxic effects of carboxylated multi-walled carbon nanotubes (MWCNTs-COOH) on zebrafish (*Danio rerio*) embryos/larvae. Chemosphere 225, 820–828.

Alak, G., Parlak, V., Ucar, A., Yeltekin, A.C., Ozgeris, F.B., Caglar, O., Atamanalp, M., Turkez, H., 2020. Oxidative and DNA damage potential of colemanite on zebrafish: brain, liver and blood. Turkish J. Fish. Aquat. Sci. 20 (8), 593–602.

Alak, G., Ucar, A., Parlak, V., Yeltekin, A.Ç., Özgeriş, F.B., Atamanalp, M., Türkez, H., 2021. Antioxidant potential of ulexite in zebrafish brain: assessment of oxidative DNA damage, apoptosis, and response of antioxidant defense system. Biol. Trace Elem. Res. 199, 1092–1099.

Alak, G., Yeltekin, A.Ç., Köktürk, M., Nas, M.S., Parlak, V., Calimli, M.H., Atamanalp, M., 2023. May PdCu@ f-MWCNT NPs be an ecotoxicologic risk? Appl. Organomet. Chem. 37 (3), e7013.

Altav, Y., Baş, A.L., Erci, F., Kocabaş, E., 2019. Veteriner hekimlikte nanoteknoloji. Dicle Üniv. Vet. Fak. Derg. 12 (2), 149–156.

Amudi, K., Yiğit, A., Menges, N., Pınar, P.T., 2023. Highly selective electrochemical sensor for new generation targeted-anticancer drug Ibrutinib using newly synthesized nanomaterial GO-NH-B (OH) 2@ AgNPs modified glassy carbon electrode. Measurement 216, 112978.

Ateş, M., Demir, V., İmamoğlu, H., 2013. Nanoparçacıkların özellikleri ve akuatik çevreye etkisi. Ziraat Mühendisliği 360, 52–59.

Audira, G., Lee, J.S., Vasquez, R.D., Roldan, M.J.M., Lai, Y.H., Hsiao, C.D., 2024. Assessments of carbon nanotubes toxicities in zebrafish larvae using multiple physiological and molecular endpoints. Chem. Biol. Interact. 392, 110925.

Baughman, R.H., Zakhidov, A.A., De Heer, W.A., 2002. Carbon nanotubes-the route toward applications. Science 297 (5582), 787–792.

Cao, Z., Wang, P., Gao, X., Shao, B., Zhao, S., Li, Y., 2019. Lycopene attenuates aluminum-induced hippocampal lesions by inhibiting oxidative stress-mediated inflammation and apoptosis in the rat. J. Inorg. Biochem. 193, 143–151.

Chowdhry, A., Kaur, J., Khatri, M., Puri, V., Tuli, R., Puri, S., 2019. Characterization of functionalized multiwalled carbon nanotubes and comparison of their cellular toxicity between HEK 293 cells and zebra fish *in vivo*. Heliyon 5 (10), e02605. https://doi.org/10.1016/j.heliyon.2019.e02605.

Cui, S.Q., Ji, X.Y., Liang, F.X., Yang, Z.Z., 2015. Ionic liquid functionalized polymer composite nanotubes toward dye decomposition. Chin. Chem. Lett. 26 (8), 942–945.

Cunha, V., Rodrigues, P., Santos, M.M., Moradas-Ferreira, P., Ferreira, M., 2018. Fluoxetine modulates the transcription of genes involved in serotonin, dopamine and adrenergic signalling in zebrafish embryos. Chemosphere 191, 954–961.

Falinski, M.M., Garland, M.A., Hashmi, S.M., Tanguay, R.L., Zimmerman, J.B., 2019. Establishing structure-property-hazard relationships for multi-walled carbon nanotubes: the role of aggregation, surface charge, and oxidative stress on embryonic zebrafish mortality. Carbon 155, 587–600.

Ferreira, F.V., Francisco, W., de Menezes, B.R.C., Cividanes, L.D.S., dos Reis Coutinho, A., Thim, G.P., 2015. Carbon nanotube functionalized with dodecylamine for the effective dispersion in solvents. Appl. Surf. Sci. 357, 2154–2159.

Gajhede, M., Larsen, S., Rettrup, S., 1986. Electron density of orthoboric acid determined by X-ray diffraction at 105 K and ab initio calculations. Acta Crystallogr. Sect. B: Struct. Sci. 42 (6), 545–552.

Han, W., Bando, Y., Kurashima, K., Sato, T., 1999. Boron-doped carbon nanotubes prepared through a substitution reaction. Chem. Phys. Lett. 299 (5), 368–373.

Handuja, S., Srivastava, P., Vankar, V.D., 2009. Structural modification in carbon nanotubes by boron incorporation. Nanoscale Res. Lett. 4, 789–793.

Huang, Y.P., Lin, I.J., Chen, C.C., Hsu, Y.C., Chang, C.C., Lee, M.J., 2013. Delivery of small interfering RNAs in human cervical cancer cells by polyethylenimine-functionalized carbon nanotubes. Nanoscale Res. Lett. 8, 1–11.

Irani, M., Jacobson, A.T., Gasem, K.A., Fan, M., 2017. Modified carbon nanotubes/tetraethylenepentamine for CO_2 capture. Fuel 206, 10–18.
John, J.P., TE, M.N., TK, B.S., 2021. A comprehensive review on the environmental applications of graphene–carbon nanotube hybrids: recent progress, challenges and prospects. Mater. Adv. 2 (21), 6816–6838.
Junaid, M., Khir, M.M., Witjaksono, G., Tansu, N., Saheed, M.S.M., Kumar, P., Usman, F., 2020. Boron-doped reduced graphene oxide with tunable bandgap and enhanced surface plasmon resonance. Molecules 25 (16), 3646.
Jung, Y.J., Muneeswaran, T., Choi, J.S., Kim, S., Han, J.H., Cho, W.S., Park, J.W., 2024. Modified toxic potential of multi-walled carbon nanotubes to zebrafish (*Danio rerio*) following a two-year incubation in water. J. Hazard. Mater. 462, 132763.
Khalili, S., Ghoreyshi, A.A., Jahanshahi, M., Pirzadeh, K., 2013. Enhancement of carbon dioxide capture by amine-functionalized multi-walled carbon nanotube. Clean–Soil Air Water 41 (10), 939–948.
Köktürk, M., Yildirim, S., Yiğit, A., Ozhan, G., Bolat, İ., Alma, M.H., Atamanalp, M., 2022. What is the eco-toxicological level and effects of graphene oxide-boramidic acid (GO-ED-BA NP)?: in vivo study on Zebrafish embryo/larvae. J. Environ. Chem. Eng. 10 (5), 108443.
Köktürk, M., Yildirim, S., Atamanalp, M., Kiliçlioğlu, M., Ucar, A., Ozhan, G., Alak, G., 2023. Mitigation potential of zingerone and rutin on toxicity mechanisms of nickel to zebrafish based on morphological, DNA damage and apoptosis outcome analysis. J. Trace Elem. Med. Biol. 80, 127268.
Kokturk, M., Yıldırım, S., Calimli, M.H., Nas, M.S., Ibaokurgil, F., Ozhan, G., Alak, G., 2023. Perspective on green synthesis of RP-Pd/AC NPs: characterization, embryonic and neuronal toxicity assessment. Int. J. Environ. Sci. Technol. 20 (1), 871–882.
Lee, M.S., Lee, S.Y., Park, S.J., 2015. Preparation and characterization of multi-walled carbon nanotubes impregnated with polyethyleneimine for carbon dioxide capture. Int. J. Hydrog. Energy 40 (8), 3415–3421.
Liu, L., Ye, Z., 2009. Effects of modified multi-walled carbon nanotubes on the curing behavior and thermal stability of boron phenolic resin. Polym. Degrad. Stab. 94 (11), 1972–1978.
Liu, Y., Yan, X., Xing, Y., Zhao, P., Liu, M., Zhu, Y., Zhang, Z., 2024. Electrochemical and colorimetric dual-channel biosensor based on B and N co-doped carbon nanotubes. Microchem. J. 197, 109770.
Lotfipanah, S., Zeinali, M., Yaghmaei, P., 2019. Induction of caspase-2 gene expression in carboxyl-functionalized carbon nanotube-treated human T-cell leukemia (Jurkat) cell line. Drug Chem. Toxicol. 44 (4), 394–399. https://doi.org/10.1080/01480545.2019.1609025.
Maleki, A., Hamesadeghi, U., Daraei, H., Hayati, B., Najafi, F., McKay, G., Rezaee, R., 2017. Amine functionalized multi-walled carbon nanotubes: single and binary systems for high capacity dye removal. Chem. Eng. J. 313, 826–835.
Mehrbeheshti, N., Esmaili, Z., Ahmadi, M., Mooṣavi, M., 2022. A dose response effect of oral aluminum nanoparticle on novel object recognition memory, hippocampal caspase-3 and MAPKs signaling in mice. Behav. Brain Res. 417, 113615.
Ménard-Moyon, C., Venturelli, E., Fabbro, C., Samorì, C., Da Ros, T., Kostarelos, K., Bianco, A., 2010. The alluring potential of functionalized carbon nanotubes in drug discovery. Expert Opin. Drug Discov. 5 (7), 691–707.
Niu, W., Pakhira, S., Marcus, K., Li, Z., Mendoza-Cortes, J.L., Yang, Y., 2018. Apically dominant mechanism for improving catalytic activities of N-doped carbon nanotube arrays in rechargeable zinc–air battery. Adv. Energy Mater. 8 (20), 1800480.
Precourt, L.-P., Seidman, E., Delvin, E., Amre, D., Deslandres, C., Dominguez, M., Sinnett, D., Levy, E., 2009. Comparative expression analysis reveals differences in the regulation of intestinal paraoxonase family members. Int. J. Biochem. Cell Biol. 41 (7), 1628–1637.
Rahimi, K., Riahi, S., Abbasi, M., Fakhroueian, Z., 2019. Modification of multi-walled carbon nanotubes by 1, 3-diaminopropane to increase CO_2 adsorption capacity. J. Environ. Manag. 242, 81–89.
Redlich, P., Loeffler, J., Ajayan, P.M., Bill, J., Aldinger, F., Rühle, M., 1996. B C N nanotubes and boron doping of carbon nanotubes. Chem. Phys. Lett. 260 (3–4), 465–470.
Rodrigues, P., Cunha, V., Oliva-Teles, L., Ferreira, M., Guimarães, L., 2020. Norfluoxetine and venlafaxine in zebrafish larvae: single and combined toxicity of two pharmaceutical products relevant for risk assessment. J. Hazard. Mater. 400, 123171.
Sankaran, M., Viswanathan, B., 2007. Hydrogen storage in boron substituted carbon nanotubes. Carbon 45 (8), 1628–1635.
Sawant, S.V., Banerjee, S., Patwardhan, A.W., Joshi, J.B., Dasgupta, K., 2020. Synthesis of boron and nitrogen co-doped carbon nanotubes and their application in hydrogen storage. Int. J. Hydrog. Energy 45 (24), 13406–13413.
Sharma, A., Patwardhan, A., Dasgupta, K., Joshi, J.B., 2019. Kinetic study of boron doped carbon nanotubes synthesized using chemical vapour deposition. Chem. Eng. Sci. 207, 1341–1352.
Shen, J., Huang, W., Wu, L., Hu, Y., Ye, M., 2007. Study on amino-functionalized multiwalled carbon nanotubes. Mater. Sci. Eng. A 464 (1–2), 151–156.
Silva, W.M., Ribeiro, H., Seara, L.M., Calado, H.D., Ferlauto, A.S., Paniago, R.M., Silva, G.G., 2012. Surface properties of oxidized and aminated multi-walled carbon nanotubes. J. Braz. Chem. Soc. 23, 1078–1086.
Şişman, T., Geyikoğlu, F., 2010. PCB 126'ya Maruz Kalmiş Zebra Baliği (*Danio rerio*) Larvalarindaki Sensorimotor Hasarlar. TÜBAV Bilim Dergisi 3 (1), 61–66.
Song, N., Zhang, Y., Ren, S., Wang, C., Lu, X., 2022. Rational design of conducting polymer-derived tubular carbon nanoreactors for enhanced enzyme-like catalysis and total antioxidant capacity bioassay application. Anal. Chem. 94 (33), 11695–11702.
Sulukan, E., Köktürk, M., 2023. Karışım herbisitlerin (halauxifen methyl+ pyroxsulam+ cloquintocet asit) in vivo toksisitesi: zebra baliği embriyo ve larva modeli. J. Inst. Sci. Technol. 13 (1), 617–627.
Türkez, H., Geyikoğlu, F., Yousef, M.I., Toğar, B., Vançelik, S., 2013. Propolis alleviates 2, 3, 7, 8-Tetrachlorodibenzo-p-dioxin-induced histological changes, oxidative stress and DNA damage in rat liver. Toxicol. Ind. Health 29 (8), 677–685.
Turkez, H., Arslan, M.E., Tatar, A., Mardinoglu, A., 2021. Promising potential of boron compounds against Glioblastoma: in Vitro antioxidant, anti-inflammatory and anticancer studies. Neurochem. Int. 149, 105137.
Ucar, A., Yeltekin, A.Ç., Köktürk, M., Calimli, M.H., Nas, M.S., Parlak, V., Atamanalp, M., 2023. Has PdCu@ GO effect on oxidant/antioxidant balance? Using zebrafish embryos and larvae as a model. Chem. Biol. Interact. 378, 110484.
Wan, S., Bi, H., Sun, L., 2016. Graphene and carbon-based nanomaterials as highly efficient adsorbents for oils and organic solvents. Nanotechnol. Rev. 5 (1), 3–22.
Wang, F., Song, S., Li, K., Li, J., Pan, J., Yao, S., Zhang, H., 2016. A "solid dual-ions-transformation" route to s, n co-doped carbon nanotubes as highly efficient "metal-free" catalysts for organic reactions. Adv. Mater. (Deerfield Beach, Fla.) 28 (48), 10679–10683.
Yang, K., Gu, M., Guo, Y., Pan, X., Mu, G., 2009. Effects of carbon nanotube functionalization on the mechanical and thermal properties of epoxy composites. Carbon 47 (7), 1723–1737.
Yigit, A., Pınar, P.T., Akinay, Y., Alma, M.H., Menges, N., 2021. Nanotube-boramidic acid derivative for dopamine sensing. ChemistrySelect 6 (24), 6302–6313.
Zhang, D., Shi, L., Fang, J., Li, X., Dai, K., 2005. Preparation and modification of carbon nanotubes. Mater. Lett. 59 (29–30), 4044–4047.
Zhang, Y., Wu, J., Zhang, S., Shang, N., Zhao, X., Alshehri, S.M., Bando, Y., 2022. MOF-on-MOF nanoarchitectures for selectively functionalized nitrogen-doped carbon-graphitic carbon/carbon nanotubes heterostructure with high capacitive deionization performance. Nano Energy 97, 107146.
Zhao, Z., Laps, S., Gichtin, J.S., Metanis, N., 2024. Selenium chemistry for spatio-selective peptide and protein functionalization. Nat. Rev. Chem. 8 (3), 211–229.
Zohdi, S., Anbia, M., Salehi, S., 2019. Improved CO_2 adsorption capacity and CO_2/CH_4 and CO_2/N_2 selectivity in novel hollow silica particles by modification with multi-walled carbon nanotubes containing amine groups. Polyhedron 166, 175–185.